Further Insight into the Mechanism of Poly(styrene-co-methyl methacrylate) Microsphere Formation

Samantha I. Applin[1], Russell C. Schmitz[2], Pacita I. Tiemsin[3], Jan Genzer[2], John W. Connell[3], Christopher J. Wohl[3]

[1]Department of Applied Science, The College of William & Mary, Williamsburg, VA, 23185, USA

[2]Department of Chemical & Biomolecular Engineering, North Carolina State University, Raleigh, NC, 27695, USA

[3]NASA Langley Research Center, Hampton, VA, 23681, USA

ABSTRACT

Polymeric microspheres have been utilized in a broad range of applications ranging from chromatographic separation techniques to analysis of air flow over aerodynamic surfaces. The preparation of microspheres from many different polymer families has consequently been extensively studied using a variety of synthetic approaches. Although there are a variety of methods of synthesis for polymeric microspheres, free-radical initiated emulsion polymerization is one of the most common techniques. In this work, poly(styrene-co-methyl methacrylate) microspheres were synthesized via surfactant-free emulsion polymerization. The effect of co-monomer composition and addition time on particle size distribution, particle formation, and particle morphology were investigated. Particles were characterized using dynamic light scattering (DLS) and scanning electron microscopy (SEM) to gain further insight into particle size and size

distributions. Reaction kinetics were analyzed alongside of characterization results. A particle formation mechanism for poly(styrene-co-methyl methacrylate) microspheres was proposed based on characterization results and known reaction kinetics.

KEYWORDS: polystyrene, methylmethacrylate, microspheres, emulsion polymerization, particle formation

INTRODUCTION

Polystyrene latex microspheres (PSLs) are utilized in applications ranging from high-performance chromatography column packing materials to seeding materials for airflow velocity measurements in wind tunnels, as well as in drug-delivery and other biomedical purposes [1-6]. NASA has particular interest in these meso-scaled materials due to their ubiquitous use, low production cost and complexity, and the large number of nearly geometrically identical particles that can be produced. The broad range of applications of polymeric microspheres has led to an extensive investigation of their synthesis, characterization, and properties for diverse uses. One method of synthesis is free-radical initiated emulsion polymerization, which uses monomers, a radical initiator, a dispersion medium, and other stabilizers to contain particles formed during polymerization [7]. A common type of emulsion polymerization utilized for generating microspheres is surfactant-free emulsion polymerization (SFEP), which does not require additional stabilizers and has been previously investigated for styrene or methylmethacrylate (MMA). Without the use of additional reactants, SFEP is a facile technique for synthesizing microspheres with low levels of impurities and relatively low cost. In SFEP, dissolved monomers are polymerized by a radical initiator in the dispersion medium, which often contains an electrolyte to modulate repulsive interactions between like-charged species during particle formation.

Three main stages occur through the course of PSL synthesis by SFEP. Interval I (or the pre-nucleation phase) begins once the initiator is introduced into the system, where dissolved monomers immediately interact with the initiator radicals to form growing oligomeric species. In Interval I, monomer is present as droplets dispersed in the aqueous phase. Droplet size is determined by monomer solubility in the dispersion medium and other reaction conditions such as the shear rate of the mixture. As dissolved monomers react with growing radical species, monomer diffuses out of the droplets, maintaining a saturated aqueous phase. The saturation concentration, or $[M]_{sat}$, for styrene and MMA are 0.003 M and 0.150 M, respectively. When the size and number of oligomeric species become large enough, a significant number of polymer particles rapidly precipitate out of solution. The appearance of these particles marks the end of Interval I. Interval II contains three phases: an aqueous continuous phase, growing polymer particles, and monomer droplets. Throughout Interval II, the concentration of dissolved monomer remains constant as monomer diffuses out of the droplets to interact with available reactive sites in solution (i.e., growing oligomeric species, precursor particle species, small particles formed, etc.). The transition from Interval II to Interval III is characterized by the depletion of free monomer in the system. This occurs due to monomer undergoing polymerization reactions or the preferential partitioning into particles themselves, swelling of the particles to the particle monomer saturation concentration, or C_M. One distinction should be made with regards to the presence of monomer droplets in Interval III. Although there is no free monomer present, droplets comprised of oligomers or polymers are still present. These droplets are converted from monomer sources into very large particles due to polymerization reactions within the monomer droplets. As a result, they become depleted of monomer and, ultimately, are present in the final material as particles with

significantly larger diameters, i.e., often twice as large as the average particle diameter calculated from particles generated through nucleation and coagulation processes.

Adopting terminology from previous research investigating emulsion polymerization mechanisms, primary particles will be defined as particles that have been generated as a result of agglomerated species growing beyond a solubility limit, i.e., a newly precipitated particle coagulates from a stable, suspended state. Primary particle growth, then, can occur by agglomeration of primary particles, adsorption of free oligomeric species, or swelling with monomer. Polymerization conditions will be categorized by two distinct reaction environments, namely, monomer-starved and monomer-saturated conditions [8-11], where particular attention will be paid to observed secondary nucleation in the system. Secondary nucleation is characterized as the formation or presence of "new" particles at later polymerization times, which may result in a bimodal distribution of particle sizes. In a monomer-starved environment, secondary nucleation is rarely observed. This happens because solubilized oligomer or precursor particles are taken up by existing polymer particles. However, in monomer-saturated conditions, secondary nucleation is likely to be observed due to greater solubilized monomer and oligomer concentrations. This is a direct result of the rate of primary particle coagulation, R_{coag}, during nucleation exceeding the rate of primary particle generation, R_{gen}, leading to a greater tendency for primary particles to coagulate or coalesce rather than nucleate. Sajjadi et. al. have shown that conducting semi-continuous SFEP mitigates secondary nucleation under certain reaction conditions (Eq. 1) [8].

$$\frac{\partial N_P}{\partial t} = R_{gen} - R_{coag} \tag{1}$$

Equation 1 describes the rate of primary particle formation, where R_{gen} is the rate of primary particle generation and R_{coag} is the rate of primary particle coagulation. A reduction in the rate of primary particle coagulation (i.e., $R_{gen} > R_{coag}$), such as through semi-continuous SFEP, leads to a greater number of primary particles and an increase in the total number of particles present at the end of Interval II [12, 13]. The converse is more likely to be true in a monomer-saturated environment ($R_{coag} > R_{gen}$) and changes to other reaction variables, such as a reduction in the initiator concentration, must be implemented to prevent secondary nucleation [14]. A more detailed description of pertinent equations regarding monomer-starved and monomer-saturated conditions, as well as secondary nucleation (for different copolymer systems), can be found in the literature [8-18].

In this work, poly(styrene-co-methyl methacrylate) microspheres were synthesized via SFEP utilizing potassium persulfate (KPS) and magnesium sulfate ($MgSO_4$) as the initiator and electrolyte species (which acts to mediate interactions between electrostatically stabilized species), respectively. KPS decomposition kinetics are well known [19, 20] and differ from other initiators previously used in SFEP, such as V-50 [or 2,2'-azobis(2-methylpropionamide)dihydrochloride, Wako Pure Chemical Industries, Ltd.], which is soluble in organic media, and TEMPO [or (2,2,6,6,-tetramethylpiperidin-1-yl)oxyl], a stable radical often used in living radical polymerization reactions. The rate of KPS thermal decomposition is accelerated at high temperatures and low pH [21]. Particle formation mechanisms for the two-monomer system consisting of styrene and MMA were investigated through changes in monomer composition and monomer addition times, relative to the addition time of the initiator. Analyses of particle size distributions, investigation of particle morphologies, and examination of the reaction kinetics were performed for these materials.

Adapting the generally accepted mechanism of particle formation under SFEP conditions to systems containing two or more monomers has been previously investigated. Although styrene- and MMA-only systems have been previously studied, as well as seeded poly(styrene-co-methyl methacrylate) systems, the research described in this paper aims to further contribute to understanding the mechanisms involved in particle formation for this copolymer system.

EXPERIMENTAL

Materials and Instrumentation

Styrene and methyl methacrylate (Sigma Aldrich) were distilled prior to use to remove inhibitors. Magnesium sulfate ($MgSO_4$, Johnson Matthey Electronics) and potassium persulfate (KPS, Fisher Chemical) were used as received. Molar concentrations used for $MgSO_4$ and KPS (0.0051 M and 0.0005 M, respectively) were investigated prior to conducting mechanistic studies in order to achieve a desired particle size of one micrometer (results not reported here). The relative monomer composition and addition times in hours (h) for each monomer are listed in Table 1. For the single monomer batches, half of the monomer was present at the time of initiator addition and the other half was added at the time indicated in Table 1. For the copolymer batches, any delayed monomer addition consisted of the styrene portion only. Deionized water (18 MΩ resistivity) was used for all reactions.

Table 1. Sample list and batch conditions.

Sample	Mole % Styrene	Mole % MMA	Monomer Added	Monomer Addition Time After Initiator Addition (h)
PSL 1	100	0	Styrene	0
PSL 2	100	0	Styrene	2
PSL 3	0	100	MMA	0
PSL 4	0	100	MMA	2
PSL 5	25	75	Styrene	0
PSL 6	25	75	Styrene	2
PSL 7	25	75	Styrene	6
PSL 8	50	50	Styrene	0
PSL 9	50	50	Styrene	1
PSL 10	50	50	Styrene	2
PSL 11	50	50	Styrene	4
PSL 12	50	50	Styrene	8
PSL 13	75	25	Styrene	0
PSL 14	75	25	Styrene	2

Particle size measurements were conducted on a Particle Sizing System Model 780 AccuSizer. Micrographs were collected using the JEOL JSM-5600 scanning electron microscope (SEM) at an acceleration voltage from 10-15 kV. High-resolution scanning electron micrographs were collected using a Hitachi S-5200 field emission scanning electron microscope (HRSEM). The acceleration voltage during the analysis ranged from 15-20kV. All samples utilized for SEM imaging were sputter-coated with a thin layer (~3 nm) of Au/Pd prior to analysis to improve conductivity.

Polystyrene Microsphere Synthesis

Polymer microsphere synthesis was conducted in a batch-wise process, with aqueous solution volumes of ~100 mL, similarly for the MMA only batches. A 250 mL three-necked round

bottom flask was utilized as the reaction vessel and equipped with a mechanical stir rod, condensation column, and nitrogen inlet. $MgSO_4$ was added to the reaction vessel along with the deionized water prior to sealing the reaction vessel. An inert atmosphere, N_2, was passed through the reaction vessel for a minimum of 30 minutes at a flow rate ~850 sccm (standard cubic centimeters per minute). While the reaction vessel was being purged with nitrogen, another N_2 line was used to bubble N_2 through the $MgSO_4$ solution to expedite the release of any solvated oxygen (sparging). Once sparging was complete, the N_2 line was raised above the solution for the remainder of the reaction and an N_2 flow rate of ~ 350 sccm was maintained. The desired amount of monomer and the KPS initiator solution (created by dissolving the KPS in a few mL of warm deionized water) were placed in separate, sealed, glass test tubes. Each test tube was placed under vacuum, dipped into liquid N_2 for freezing and then dipped into warm water to hasten the thawing process in order to return the contents to a liquid state for addition to the reaction vessel. All additional reactants underwent this freeze-thaw process, which was completed a minimum of three times under vacuum prior to introduction into the flask via cannula transfer. Prior to the cannula transfer of KPS initiator, the reaction vessel was heated to ~70°C (allowing time to equilibrate) and the mechanical stirrer was set to 250 rpm. All reactants introduced after purging the reaction vessel with nitrogen were added at slow stir rates (50 rpm). Reaction temperature was maintained at 70°C after the initial heating and was monitored via a thermocouple placed in the oil bath surrounding the reaction vessel. The heat source for the reaction was turned off 21 h after injecting KPS. The resultant latex solutions were collected in glass bottles after being filtered through cheesecloth to remove any excessively large agglomerates of material in the reaction mixture.

Poly(styrene-co-methyl methacrylate) Microsphere Synthesis

Poly(styrene-co-methyl methacrylate) microsphere synthesis was conducted similarly to the homopolymer systems described above. In the time study experiments, the reaction vessel was initially charged with water and MMA; styrene addition was delayed until after KPS was added. Two series of composition studies were performed. For one series, both MMA and styrene were transferred to the reaction vessel, via cannula, after sparging and prior to heating. In the secondary series, the reaction vessel was initially charged with the MMA at the same time as the first series, while the styrene was added via cannula at a specific time after the initiator addition as indicated in Table 1. The maximum delay time of 8 h was chosen as initial experiments indicated poor incorporation of styrene monomer at greater delay times. Polymerization was carried out for 21 h, after which the reaction mixture was cooled and collected with the same procedure used for homopolymer latexes.

Dynamic Light Scattering

Samples for DLS characterization were prepared by collecting ~5 mL of the filtered latex and sonicating for 10 minutes to break up particle aggregates. Approximately 200 μL of the sonicated latex was added to 40 mL of deionized water and was agitated to ensure good mixing. Approximately 200 μL of this diluted latex was added to the instrument sample volume (35 mL). The sample volume vessel was rinsed in triplicate and the analysis section was flushed in triplicate between runs to prevent contamination by previous measurement constituents. After autodilution to 10,000 particles per scan, measurements were collected over 60 seconds from 0.5 to 10 μm. The results were compiled and statistical analysis was performed to determine the mean particle diameter and standard deviation.

Microscopic Characterization of PSLs

Microsphere samples were prepared for SEM characterization by combining ~10 mL of filtered latex and 30 mL of deionized water in a centrifuge tube. The dispersion/diluted latex was sonicated for 10 minutes and then centrifuged (Thermo Scientific Sorvall ST8 Centrifuge) at 3000 rpm for 10 minutes. The sedimented particles were resuspended by adding a few milliliters of deionized water and sonicating the mixture for 10 minutes. Approximately 0.25 mL of this concentrated latex was cast onto a prepared glass slide. Slides were prepared by soaking in 5 M NaOH solution for ~10 minutes in order to increase the wettability of the slide by the latex. The PSL dispersion was spread on the slide using a pipette tip. The sample was dried under ambient conditions then sputter-coated with Au/Pd (~3 nm thickness).

SEM Image Analysis

SEM images were analyzed to determine dry PSL particle diameter for comparison with the solution-based DLS measurements, which measured hydrodynamic particle diameters. Thus, it was anticipated that SEM image analysis would measure smaller particle diameters, which has been reported previously [22, 23]. Diameters were measured for at least 100 particles (often considerably more) from at least two SEM images. As this approach relies on the image resolution for obtaining accurate diameter data, the magnification level for each batch was a crucial consideration. The PSL diameter varied considerably as a result of different reaction conditions and an acceptable scaled dimension range, R_{SD}, was devised as a way to balance image resolution with magnification level. The scaled dimension was defined as the value of the average particle diameter multiplied by the magnification of the SEM micrograph taken. An acceptable scaled

dimension range was determined to be 2500 μm ≤ R_{SD} ≤ 6000 μm. As an example, under these conditions, PSLs with an average particle diameter < 0.5 μm required an SEM magnification level equivalent to or above 5000x magnification in order to be analyzed. For comparison of different particle populations, the polymer mass for each particle size was calculated and these values summed according to a small particle diameter population (m_S, diameters ≤ 0.5 μm) and a large particle diameter (m_L, diameters > 0.5 μm). The percentage of polymer mass associated with the large particle diameter, $\%m_L$, was calculated by dividing m_L by the total of m_S and m_L (Table 2).

RESULTS & DISCUSSION

A series of poly(styrene-co-methyl methacrylate) latexes were successfully synthesized based on observed opacity changes during polymerization, as well as characterization results from SEM and DLS analyses (Table 2). With the exception of batch 7, no material was collected during filtration through cheesecloth at the completion of each particle synthesis reaction. This indicated that no large aggregates were formed, which may arise under various reaction conditions and would indicate a diminished particle generation yield. Particle mean diameter and standard deviation (std. dev.) data from DLS and SEM image analysis (SEM IA), as well as coefficient of variance (CoV) values, can be seen in Table 2. DLS provided insight into particles with diameters greater than 0.5 μm, while SEM IA provided data for the smaller diameters as well as the particle size distribution.

Assuming very similar reaction conditions, styrene, with significantly lower water solubility than MMA, would be anticipated to yield larger average particle diameters than those of MMA only systems, consistent with observations in this work. The PMMA homopolymer latexes, PSL 3 and 4, exhibited much smaller average particle diameters (0.4-0.7 μm) than the PS

homopolymer latexes, PSL 1 and 2 (0.9-1.1 μm). It was also observed that samples with stoichiometric equivalent concentrations of styrene and MMA produced particles with intermediate diameters (0.5-0.8 μm).

Table 2. Batch particle diameter data.

Sample	Composition (Sty:MMA) (mole%)	DLS Mean (μm)	SEM IA Mean (μm)	CoV DLS	CoV SEM IA	$\%m_L$
PSL 1	100 : 0	0.98 ± 0.24	0.95 ± 0.16	0.24	0.17	100
PSL 2	100 : 0	1.12 ± 0.13	1.07 ± 0.02	0.12	0.02	100
PSL 3	0 : 100	0.87 ± 0.65	0.44 ± 0.03	0.75	0.06	4
PSL 4	0 : 100	0.75 ± 0.34	0.43 ± 0.16	0.46	0.36	66
PSL 5	25 : 75	1.07 ± 1.18	0.52 ± 0.03	1.11	0.06	86
PSL 6	25 : 75	0.65 ± 0.15	0.58 ± 0.09	0.23	0.16	94
PSL 7	25 : 75	0.63 ± 0.28	0.44 ± 0.07	0.45	0.16	31
PSL 8	50 : 50	1.25 ± 1.49	0.55 ± 0.03	1.19	0.05	96
PSL 9	50 : 50	0.68 ± 0.48	0.47 ± 0.03	0.70	0.06	23
PSL 10	50 : 50	0.62 ± 0.33	0.40 ± 0.05	0.53	0.13	5
PSL 11	50 : 50	0.75 ± 0.25	0.38 ± 0.05	0.33	0.13	47
PSL 12	50 : 50	0.79 ± 0.19	0.39 ± 0.12	0.24	0.30	72
PSL 13	75 : 25	1.06 ± 1.18	0.48 ± 0.25	1.11	0.52	85
PSL 14	75 : 25	1.32 ± 1.11	0.90 ± 0.20	0.84	0.22	99

Single Monomer Formulations

SFEP using only one monomer indicated that differences in monomer properties (water solubility, reaction kinetics, etc.) resulted in significant differences in particle sizes and size distributions. When monomer was added all at once the styrene only and MMA only latexes (PSL 1 and 3) yielded mean particle diameters, according to SEM IA, of 0.95 μm and 0.44 μm, respectively. These values did not change appreciably when half of the monomer was introduced to the system 2 h after the initiator (Figure 1). The change in coefficient of variation values (CoV, the standard deviation divided by the mean), however, was contradictory for the two single monomer systems when the monomer addition was separated into two steps. For the styrene only cases (PSL 1 and 2), CoV decreased from 17 to 2% when half the monomer was added 2 h after

the initiator. Conversely, CoV increased from 7 to 36% for the MMA batches under the same monomer addition conditions (PSL 3 and 4). This suggests that, for the styrene batches, the addition of monomer in two steps prevented secondary nucleation, whereas for the MMA cases, it contributed to secondary nucleation. This can be attributed to the significantly greater water solubility and polymerization rate of MMA, relative to styrene, which would result in a greater advance in the polymerization in the MMA case (i.e., lower free monomer concentration at the time when the second addition of monomer occurred resulting in secondary nucleation and smaller, albeit a greater number, of PMMA particles). MMA polymerization rates may have also accelerated as a result of the "gel effect," an increase in the rate of polymerization due to termination reactions being diffusion-controlled [17].

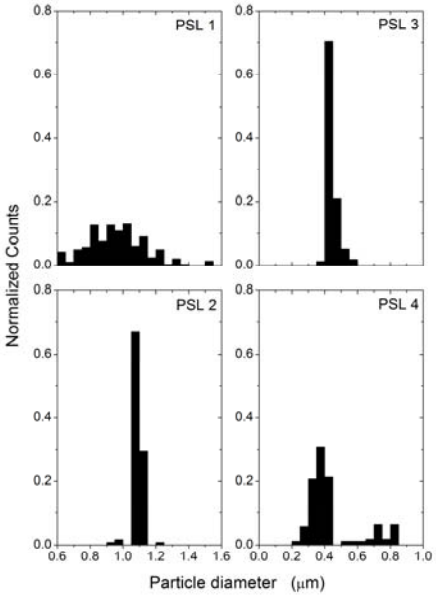

Figure 1. Particle size distribution comparison from SEM IA for styrene only latexes (PSL 1 and 2) and MMA only latexes (PSL 3 and 4).

Mixed Composition Studies

Based on monomer material properties and previous studies of SFEP kinetics for each monomer, it was expected that, under mixed monomer conditions, the MMA species would participate in considerably more reactions shortly after initiation, relative to styrene. Therefore, an approximation will be taken that the reaction kinetics of this system at times shortly after initiator addition can be described using results derived from MMA studies [24-27].

For the mixed monomer composition study conducted with same-time monomer addition (i.e., t=0 h, PSL 5, 8 and 13), it was apparent that the greater the mole percent of styrene, the larger the resultant particle diameters (Figure 2). A general agreement was found between mean particle diameters determined by DLS and by SEM IA results (Table 2). Information obtained from the DLS was limited, especially for smaller particle diameters, due to the lower detection limit of the instrument (0.5 μm) and the inability to differentiate instrument responses as arising from single particles or aggregates. Therefore, data collected from the DLS was verified using SEM IA for batches that contained larger particle diameters (i.e., a significant population > 0.5 μm); otherwise, only data obtained from SEM IA was utilized.

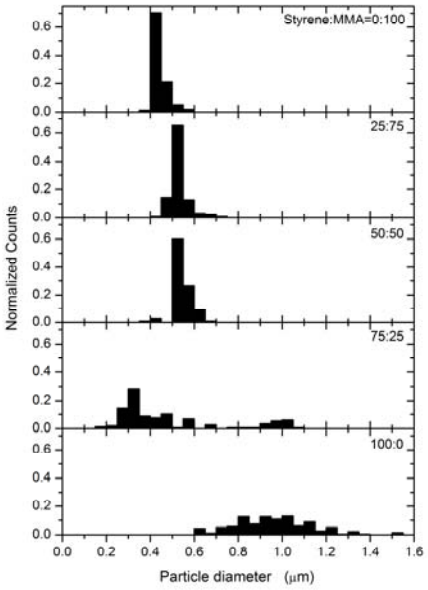

Figure 2. Particle size distribution comparison from SEM IA for composition study at t=0 h. (Data normalized and offset.)

The change in mean particle diameter followed a nonlinear relationship with monomer content. A minimum in particle diameter was observed at 75% styrene (PSL 13). Since MMA is more reactive and water soluble than styrene, it can be assumed that with higher styrene content, the rapidly generated MMA-rich particles would swell with styrene monomer up to saturation concentrations. Under these conditions, a relatively low concentration of small diameter particles are favorable for secondary nucleation [28]. This would result in generation of a large number of small particles consisting of both PMMA-enriched and PS-enriched particles. This is further suggested by the change in the CoV values. CoV values from SEM IA for the composition study with same-time monomer addition showed that the distribution broadened with increasing styrene content reaching a maximum at 75% styrene.

For the composition study conducted at 2 h delayed styrene addition, along with the time study (described below), the kinetics of MMA become even more pertinent in understanding resultant particle formation. The concentration of MMA in solution, assuming even distribution of

monomer, [M], (i.e., MMA is not concentrated into monomer droplets), when styrene monomer is added, can be described by:

$$[M](t) = [M]_0 - \frac{\hat{x}(t)}{M_0 V} \tag{2}$$

where $[M]_0$ is the initial concentration, $\hat{x}(t)$ is the amount of MMA consumed as a function of time after the pre-nucleation period, M_0 is the molecular weight of MMA, and V is the reaction volume. This is significant as the transition from Interval II to Interval III occurs when $[M] < [M]_{sat}$, where $[M]_{sat}$ is the saturation concentration of MMA in water. For MMA in water, the concentration is: $[M]_{sat} = 0.150$ M [25]. Thus, after the MMA concentration has fallen below $[M]_{sat}$, addition of styrene should result in, monomer-saturated conditions and secondary nucleation, demonstrated as a bimodal particle size distribution. For same-time monomer addition, using only 25 mole percent MMA, the initial MMA concentration was already below $[M]_{sat}$ (PSL 5). Due to the relatively low reactivity and low water solubility of styrene (in comparison to MMA), secondary nucleation was not observed in this batch; instead, the nucleated particles swell with monomer throughout the polymerization. It should be noted that secondary nucleation can occur under similar conditions with the initially generated PMMA particles sufficiently dilute and the presence of a surfactant [29].

The kinetics of emulsion polymerization as described in the work of Ballard, et. al. [25] were used to estimate the time at which $[M] < [M]_{sat}$. From their work [25], the rate of MMA consumption was defined as:

$$\frac{d\hat{x}}{dt} = \frac{N_c}{N_A} k_P M_0 C_M n(t) \tag{3}$$

where N_c is the number of seed particles present, N_A is Avogadro's number, k_P is the rate of polymerization, C_M is the concentration of monomer in the seed particles, and n(t) is the number of free radicals in each particle as a function of time. Considering first N_c, in the work of Ballard, the kinetics were determined by starting with seed PMMA particles, ~50 nm in diameter. For the work described here, no seed particles were used. Tauer, et. al. studied the kinetics of SFEP of styrene and concluded that the initial particle concentration at the end of the pre-nucleation phase (Interval I) was $\sim 1.76\times10^{13}$ particles/mL and that the pre-nucleation phase lasted ~430 s [26]. In their work, the total dissolved monomer concentration necessary to support this number of particles was below the saturation concentration of styrene in water. Therefore, this is a starting point for predicting the number of particles generated in the work described here, as well as a similar time requirement to transition from Interval I to Interval II. Thus, as a first approximation, $N_c = 1\times10^{13}$ will be used and the calculated times will be increased by 400 s to account for the duration of Interval I. Next, although k_P is dependent upon the weight fraction (w_P) of monomer and in a particle, it is assumed that above the T_g (50°C at w_P ~0.8) [27], this dependence is removed. Therefore, k_P was assumed to be constant and the value of 580 $M^{-1}s^{-1}$ reported in Ballard's work will be utilized here. Although Ballard determined that the Interval II polymerization kinetics were not steady state, for the purpose of the estimation here, steady state kinetics are assumed. Therefore, a constant C_M and n of 6.6 M and 0.5, respectively, are used here [25]. The right-hand-side of equation 3 can be approximated as a series of constants, which when integrated provides a linear relationship between time and the amount of monomer consumed. Based on this approach, the time required for [M] to fall below $[M]_{sat}$, t_{trans}, was determined for each reaction condition (Table 3). The transition times between Interval II and III were scaled to

account for the observations from the time study samples (PSL 8-12, Table 1) by dividing the times by a scaling factor (0.5) to enable prediction as described later.

Table 3. Calculated Interval II to Interval III transition times.

MMA Monomer (mole%)	$[MMA]_0$ (M)	t_{trans} (min)
25	0.146	0
50	0.291	160
75	0.437	310
100	0.582	480

Based on these times and the assumption that the reaction will transition from Interval II to Interval III when $[M] < [M]_{sat}$, secondary nucleation (i.e., monomer-saturated conditions) should be observed when styrene is introduced after t_{trans}. In the composition study with two-hour delayed styrene addition (PSL 2, 4, 6, 10, and 14), when $[M] \geq [M]_{sat}$, a relationship between monomer composition and particle size was not evident, although, with the increase in styrene, the particle diameters seemed to increase from PSL 6 to PSL 14 (Table 2). Comparing characterization data and previously described reaction kinetics associated with the transition from Interval II to III, it was concluded that the smaller mean particle diameter in PSL 10, compared to PSL 6, was a result of the increase in the total number of new particles generated shortly after monomer addition events with less monomer swelling in comparison to PSL 6. In other words, stable PMMA particles were formed before the delayed addition of styrene in both batches. Any styrene added after two hours was incorporated into the stable particles, either by swelling with monomer or by adsorption of oligomers and precursor particles onto the stable particle surface. In PSL 10, more MMA initially present in solution enabled more new particles to be nucleated and stabilized than in PSL 6, ultimately resulting in smaller particles (Figure 3).

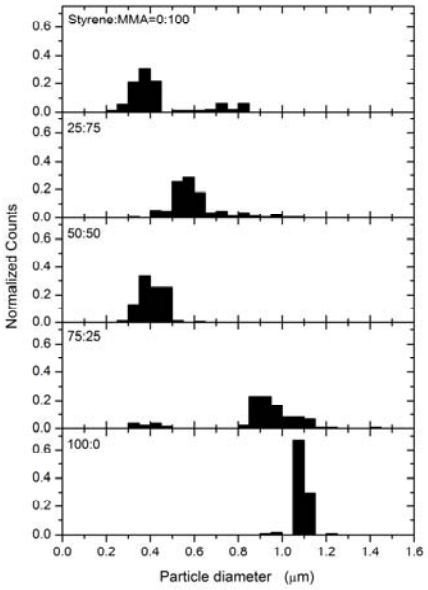

Figure 3. Particle size distribution comparison from SEM IA for composition study at t=2 h (i.e., two-hour styrene addition after initiator). (Data normalized and offset.)

Based on calculated values of t_{trans} (Table 3) and kinetic assumptions as described previously, no major differences in size distribution would be expected between the 75:25 styrene:MMA batches (PSL 13 and 14) for styrene addition at t=0 or t=2 h. This is because the initial [MMA] was below $[M]_{sat}$, suggesting that the system, with respect to the MMA monomer, would have transitioned rapidly to Interval III. The Interval III PMMA particles would have acted as seed particles for emulsion polymerization of styrene. This was observed with the average particle diameters for PSL 13 and 14, determined to be 1.056 and 1.321 μm (DLS diameters), respectively (Figure 4). Data collected for these batches via SEM IA indicated a significant difference in particle size which indicates that secondary nucleation may have also occurred in PSL 13 as a result of the relatively low number of small diameter PMMA seed particles that would have been generated rapidly prior to significant conversion of styrene monomer. This can be seen in the difference in particle size distributions between these two batches (Figures 2 and 3), with PSL 13 having a greater population of small diameter particles, relative to PSL 14. It should be

noted though that the polymer mass in the small population, m_S, of PSL 13 is still relatively low ($\%m_L$ for PSL 13 and 14 was approximately 85% and 99%, respectively) indicating that secondary nucleation was not a major styrene monomer reaction pathway.

Differences in morphology were also observed between PSL 13 and 14, which was attributed to the delayed addition of styrene. In PSL 14, styrene was introduced closer to t_{trans} and it is assumed that the apparent surface roughness of the particles is due to coalescence of precursor particles onto the surface of a larger, more stable particle without additional monomer swelling. Had monomer swelling occurred, the increase in polymer chain mobility would have enabled reconfiguration to a more stable, smooth spherical morphology [22].

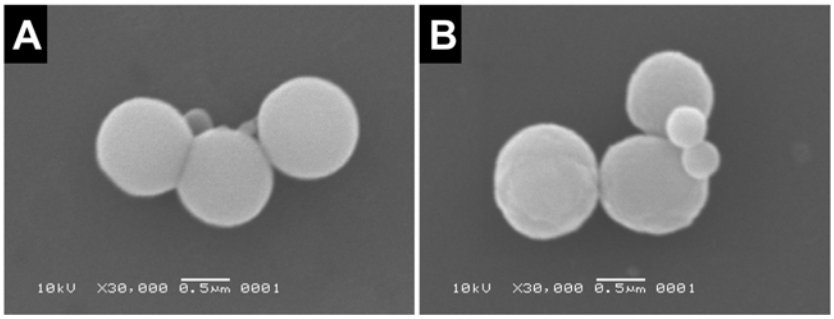

Figure 4. Scanning electron micrographs of PSL 13 (A) and 14 (B).

Another expected result for PSL batches of 25:75 styrene:MMA (PSL 5 and 6), where the styrene was added at either t=0 or t=2 h, was a nominal difference in size distributions due to [MMA] at the time of styrene addition being greater than $[M]_{sat}$. This would indicate that the system, with respect to the MMA monomer, would have persisted in Interval II for the delayed additions of styrene investigated here and minimal secondary nucleation should have occurred. This was verified by SEM images (Figure 5).

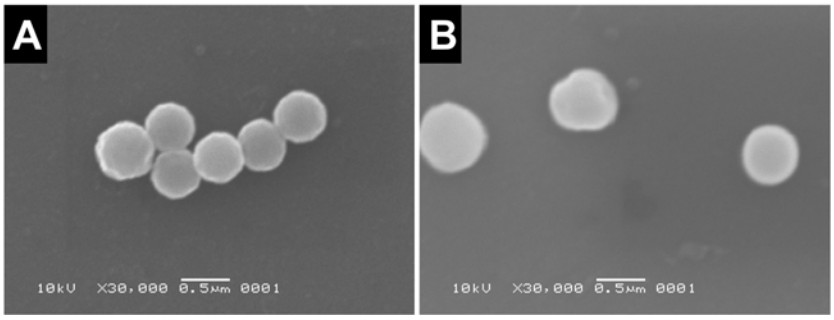

Figure 5. Scanning electron micrographs of PSL 5 (A) and 6 (B).

The particles synthesized in PSL 5 and 6, containing more MMA than styrene, exhibited relatively rough particle morphologies, while particles from PSL 13 (containing more styrene than MMA) were smoother (Figure 4 vs. Figure 5). This may be attributed to the lower reactivity and lower water solubility of styrene, in relation to MMA, which would lead to greater monomer swelling of growing particles and formation of a more thermodynamically favorable, smooth morphology. Conversely, with a greater MMA content, the rapid nucleation and coalescence of small particles would lead to rougher particle morphologies (Figure 6).

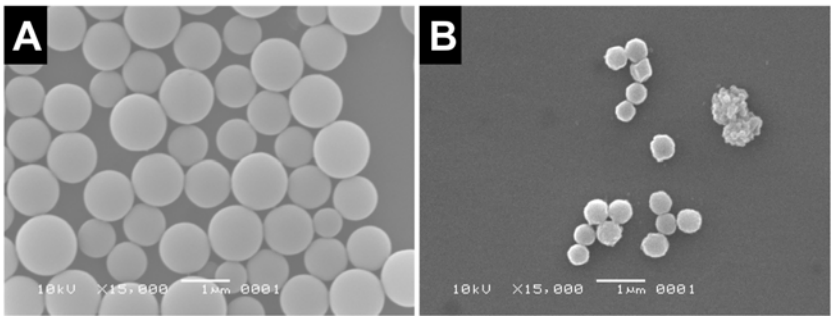

Figure 6. Scanning electron micrographs of PSL 1, styrene only (A), and 3, MMA only (B).

Styrene Addition Time Study

For the time study conducted at 50:50 styrene:MMA, which evaluated the impact of styrene addition before or after $[M] < [M]_{sat}$, secondary nucleation (i.e., bimodal size distribution) was observed in batches where the styrene addition was delayed after this transition (PSL 11 and 12).

This was verified by SEM with the clear observation of two populations of particles for styrene addition times greater than 2 h (Figure 7). With the great disparity in particle diameter between these two populations of particles, both DLS and SEM IA data were used to evaluate the full range of particle diameters present (Figure 8).

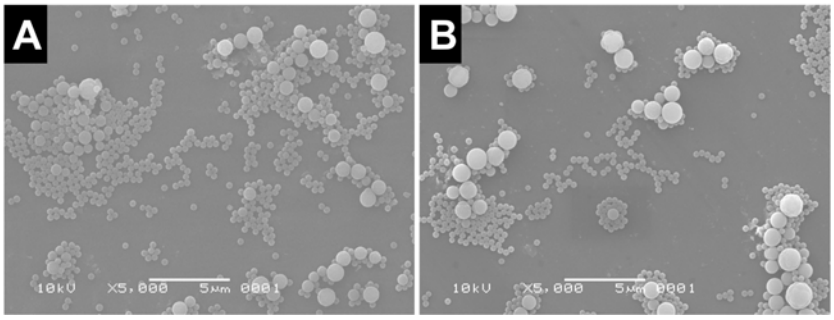

Figure 7. Scanning electron micrographs of PSL 11 (A) and 12 (B).

Based on SEM IA (Table 2, Figure 8), the mean particle diameter of the small diameter particle population decreased as styrene was introduced into the system later in the polymerization, whereas, the DLS data exhibited an increase in average particle diameter. With later styrene addition, the standard deviation and CoV values for DLS data gradually decreased but increased for SEM IA data (Figure 8, Table 2). These observations can be attributed to secondary nucleation (i.e., generating particles too small to be detected by the DLS instrument used in this work) becoming a more dominant pathway for polymerization as the styrene addition time increased.

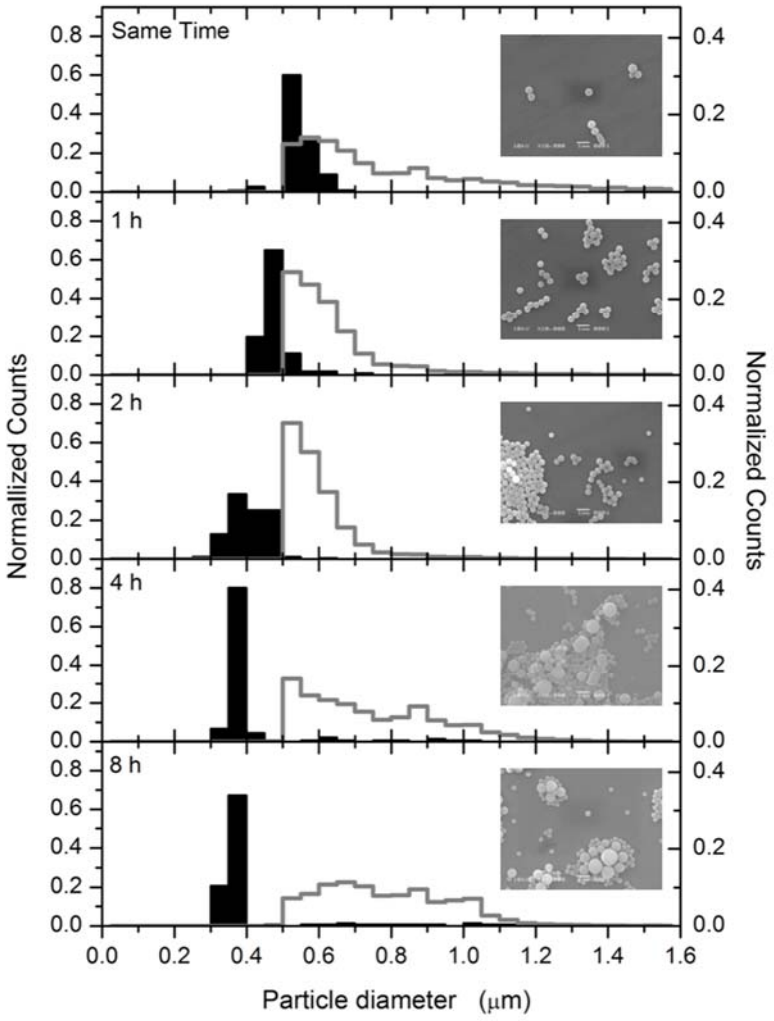

Figure 8. Normalized particle size distribution comparison from SEM IA (black, filled bars) and DLS (gray, open bars) data for PSL 8-12 (from top to bottom).

When styrene was introduced prior to $[M] < [M]_{sat}$ (PSL 8, 9, and 10), no secondary nucleation was observed. In PSL 8, the same-time monomer addition case (for which the reaction behavior has been discussed previously in this paper, see *Mixed Composition Studies*), particle diameters appeared to be uniformly distributed around a single mean (0.55 μm) with a few observed anomalous particles. SEM IA mean particle diameter was larger than in MMA only batches but half the size of styrene only batches synthesized under these conditions. As the

diameter was larger than the MMA only batches, the relative polymer mass associated with larger diameter particles ($\%m_L$ = 96%, Table 2) indicated that the particles would likely be comprised of both monomer types. Moreover, the SEM IA standard deviation was small, verifying the uniformity in this sample. This result can be related to the likelihood that, at this MMA concentration, a large number of PMMA particles were rapidly generated suppressing secondary nucleation events for the remaining, slower reactivity styrene monomer (28). For PSL 9, where the styrene was introduced 1 h after the initiator, the mean particle diameter was smaller than PSL 8 with little changes in the standard deviation measured by SEM IA. This decrease in mean particle diameter (described by SEM IA data) may be attributed to an increase in the number of PMMA particles formed prior to the addition of styrene, which was added when $[M] > [M]_{sat}$. The $\%m_L$ value (23%) was less than PSL 8, which is further evidence of a greater number of PMMA particles being present at the time of styrene addition. Analysis of DLS and SEM IA data for PSL 10 (styrene addition at two hours after initiator addition) clearly indicated the presence of two particle populations. Interestingly, the $\%m_L$ value was the lowest for this batch, 5%. This indicated the likelihood that even more PMMA particles had formed, relative to PSL 9, at the time of styrene addition. Furthermore, for PSL 10, since styrene monomer was introduced close to t_{trans} (see Table 3, 50% MMA), the lack of appearance of a bimodal size distribution supports the validity of the assumptions made in the reaction kinetics analysis. The observation that the nearly monodisperse size distribution was accompanied by a reduction in $\%m_L$ were utilized to scale the reaction kinetics described above. By inclusion of a scaling factor of 0.5 to the calculated transition time between Interval II and III based on these observations, transition times for other copolymer particle synthesis formulations can be predicted.

The DLS and SEM IA mean particle diameters increased from PSL 11 to 12, which suggests that more monomer swelling occurred in PSL 12 after MMA and styrene particles had been nucleated. Furthermore, the mean particle diameter in PSL 12, determined from DLS data, more closely resembled styrene only diameters than PSL 11, which may indicate that the two particle populations seen in these characterizations could be related to the two monomers present. In other words, the larger particle population resembled styrene only particle diameters, i.e., the addition of styrene monomer could be interpreted as a secondary nucleation event, while the smaller particles resembled those of MMA only particle diameters. However, DLS was unable to detect the smaller particle population, observed during SEM IA, which caused the decrease in standard deviation from PSL 11 to 12 in the DLS data. SEM IA was able to measure the smaller particle size distribution for these samples and indicated an increase in the standard deviation. The overall particle size distribution as determined by SEM IA, further indicated that significant secondary nucleation was occurring as would be expected assuming that the styrene addition occurred well after the approximated transition time from Interval II to III. This is further verified by an increase in $\%m_L$ for these two batches (47% and 72%, respectively) suggesting fewer particles and secondary nucleation, consistent with expected results of the addition of styrene to the system after transition to Interval III.

Using the predicted t_{trans} values (Table 3) and a scaling factor based on empirical results from 50:50 particle formulations, an additional batch (25:75 styrene:MMA composition), which had a predicted t_{trans} of 313 minutes (Table 3), was synthesized (PSL 7). Styrene was introduced at 6 h (360 min) after initiating the polymerization for PSL 7. A bimodal distribution, suggesting secondary nucleation, was observed in the product, as well as coagulation of these nucleated particles (Figure 9). It should be noted that PSL 7 had a significant amount of solids filtered out in

the workup process. Upon collecting the retentate for further analysis, particles or particle aggregates were visually observed in the powder-like substance remaining (Figure 9). Therefore, it can be assumed that even larger particle diameters than those observed in DLS (and SEM IA) for PSL 7 were neglected due to the removal of these particles in the workup. This would dramatically increase both the calculated mean particle diameter and CoV for this batch. Collectively, these observations demonstrated that the predicted transition time was prior to the styrene addition time.

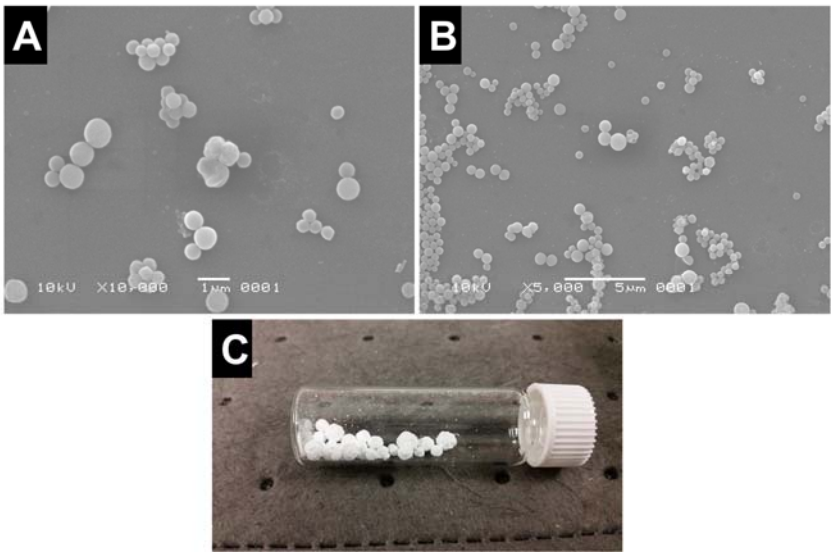

Figure 9. (A and B) Scanning electron micrographs of PSL 7, two different locations on the sample slide. (C) Image of captured particles during the workup process from PSL 7. The sample bottle is approximately 59 mm in length.

CONCLUSIONS

In this work, the synthesis of poly(styrene-co-methyl methacrylate) microspheres was conducted to help elucidate and provide further insight into particle formation mechanisms. By investigating fundamental behaviors of the individual monomers, the co-monomer system, and resultant microsphere properties obtained using DLS, SEM, and SEM IA, it was determined that the introduction of styrene later in the copolymerization increased the particle size distribution,

and the more styrene present increased the resultant mean particle diameter. Additionally, upon further analysis of the reaction kinetics between the two monomers, it was found that the time when the reaction transitioned from Interval II to Interval III (i.e., no monomer droplets present in the system) played a key role in determining resultant particle properties. Ultimately, the results of this study could be utilized to identify an optimal synthetic methodology for generation of copolymeric particles with a particle size determines *a priori*, a narrow size distribution, and controlled surface morphology.

REFERENCES

1. B. Yu, C. Tian, H. Cong, T. Xu, J. Mater. Sci. 51 (2016) 5240-5251.
2. C. J. Wohl, J. M. Kiefer, B. J. Petrosky, P. I. Tiemsin, K. T. Lowe, P. M. F. Maisto, P. M. Danehy, ACS Appl. Mater. Interfaces 7 (2015) 20714-20725.
3. J. Qu, Y. Xu, J. Liu, J. Zeng, Y. Chen, W. Zhou, J. Liu, J. Chromatography A 1441 (2016) 60-67.
4. D. Sarma, K. Gawlitza, K. Rurack, Langmuir 32 (2016) 3717-3727.
5. A. B. Serrano-Montes, J. Langer, M. Henriksen-Lacey, D. J. de Aberasturi, D. M. Solis, J. M. Taboada, F. Obelleiro, K. Sentosun, S. Bals, A. Bekdemir, F. Stellacci, L. M. Liz-Marzan, J. Phys. Chem. C 120 (2016) 20860-20868.
6. S. L. Sonawane, S. K. Asha, ACS Appl. Mater. Interfaces 8 (2016) 10590-10599.
7. S. Slomkowski, J. V. Aleman, R. G. Gilbert, M. Hess, K. Horie, R. G. Jones, P. Kubisa, I. Meisel, W. Mormann, S. Penczek, R. F. T. Stepto, Pure Appl. Chem. 83(12) (2011) 2229-2259.
8. S. Sajjadi, RSC Adv. 5 (2015) 58549-58560.
9. A. R. Goodall, M. C. Wilkinson, J. Hearn, Polymer Colloids II (1980) 629-650.
10. I. Capek, Adv. Colloid Interface Sci. 82 (1999) 253-273.
11. S. Sajjadi, Am. Institute of Chem. Eng. J. 55(12) (2009) 3191-3205.
12. F. K. Hansen, J. Ugelstad, J. Polym. Sci., Polym. Chem. Ed. 16 (1978) 1953-1979.
13. R. M. Fitch, M. B. Prenosil, K. J. Sprick, J. Polym. Sci., Part C: Polym. Symp. 27PC (1969) 95-118.
14. K. Tauer, P. Nazaran, Macromol. Symp. 288 (2010) 1-8.
15. C. S. Chern, Prog. Polym. Sci. 31 (2006) 443-486.
16. S. C. Thickett, R. G. Gilbert, Polymer 48 (2007) 6965-6991.
17. K. Tauer, H. Hernandez, S. Kozempel, O. Lazareva, P. Nazaran, Colloid Polym. Sci. 286 (2008) 499-515.
18. Y. Chen, S. Sajjadi, Polymer 50 (2009) 357-365.
19. N. M. Beylerian, L. R. Vardanyan, R. S. Harutyunyan, R. L. Vardanyan, Macromol. Chem. Phys. 203 (2002) 212-218.
20. I. M. Kolthoff, I. K. Miller, J. Am. Chem. Soc. 73 (1951) 3055-3059.

21. D. A. House, Chem. Rev. 62(3) (1962) 185-203.
22. T. Yamamoto, M. Nakayama, Y. Kanda, K. Higashitani, J. Colloid Interface Sci. 297 (2006) 112-121.
23. T. Yamamoto, Y. Kanda, K. Higashitani, J. Colloid Interface Sci. 299 (2006) 493-496.
24. S. Hsu, W. Chiu, C. Lee, H. Chang, Polym. J. 33(1) (2001) 27-37.
25. M. J. Ballard, D. H. Napper, R. G. Gilbert, J. Polym. Sci.: Polym. Chem. Edition 22 (1984) 3225-3253.
26. K. Tauer, R. Deckwer, I. Kuhn, C. Schellenberg, Colloid Polym. Sci. 277 (1999) 607-626.
27. N. Friis, A. E. Hamielec, J. Polym. Sci.: Polym. Chem. Edition 12 (1974) 251-254.
28. C. J. Ferguson, G. T. Russell, R. G. Gilbert, Polymer 43 (2002) 4557-4570.
29. B. R. Morrison, R. G. Gilbert, Macromol. Symp. 92 (1995), 13-30.